1. KEY POINTS

From the vantage point of structural dynamics and acceleration data analysis, the key points for those interested in the SpaceX Dragon reboost that took place on GMT 2026-01-23 are as shown in the bullets below.

- **Context on SAMS System** The Space Acceleration Measurement System (SAMS) sensors measure vibratory accelerations in the microgravity environment of the ISS. This report highlights their use in capturing quasi-steady and transient vibrations during reboost, which helps assess impacts on experiments and equipment sensitive to disturbances.
- **Purpose of Reboost** Dragon SpX-33's reboost maneuver counters atmospheric drag on the ISS, maintaining its orbital altitude. The reported 2.3 m/s ΔV raising the altitude by 4.34 km is typical for such operations and can be approximated as shown in Appendix B – a first-order, first-principles estimate starting from basic orbital energy relationships and keeping only the dominant effect of a small prograde ΔV, which yields our first-order approximation.
- **"Hammer Hit" Analogy** The sudden thrust impulses during settling burns are aptly described as "hammer hits." These are short-duration, high-frequency events – visible in spectrograms like Fig. 4 through Fig. 7 – that help ensure propellant settling before the main burn, preventing engine issues from gas ingestion.
- **Coordinate System** In this document – unless explicitly stated otherwise – we reference the body-fixed Space Station Analysis (SSA) coordinate system.
- **~GMT 2026-01-23/06:30** End of about a 90-minute maneuver to -XVV ("tail-forward") attitude, which orients the ISS such that its negative X direction aligns with the velocity vector, allowing the Dragon's (now aft-directed) thrusters to provide prograde thrust (along the direction of flight) for the upcoming reboost event.
- **GMT 2026-01-23/18:06** Handover from US Momentum Management to Russian Segment (RS) for attitude control. This gives tighter control and quicker response, *but at the cost of thruster firings* instead of control moment gyros (CMGs). Such RS firings tend to excite low-frequency structural vibrations below about 2-3 Hz.
- **GMT 2026-01-23/18:35** Start of about 3-minutes duration of settling burn pulses (once every 5 seconds, a total of 18 pulses) by the Dragon vehicle thrusters. For these 3 minutes, due to their 5-sec period, we see this stimulus give rise to short-lived, global structural mode vibrations (particularly the main truss "mode one" near 0.1 Hz) and produce distinctive odd harmonics (0.1, 0.3, 0.5, 0.7, 0.9, ... up to ~20 Hz) in the SAMS measured response throughout the ISS.
- **GMT 2026-01-23/18:38:21** At this time, just after the 18th settling burn pulse, the Dragon started continuously firing thrusters for another ~23 minutes 8 seconds – the remainder of the reboost event.
- **GMT 2026-01-23/19:23** Handover from RS to US Momentum Management for attitude control. This resumes typical attitude control via CMGs.
- **~GMT 2026-01-23/23:30** Begin ~90-minute maneuver to +XVV (nominal) attitude.
- The analysis in this document focuses on SAMS data, using time–frequency spectrogram and interval-averaged acceleration visualizations. Together, these plots provide insight into the reboost and related events. Calculations based on SAMS measurements show that the flight controllers' prediction of 2.405 m/s for the desired ΔV was nearly achieved via a negative X-axis step with a steady-state, ~23-minute plateau of roughly -0.17 mg. This resulted in a SAMS-measured estimated ΔV of about 2.31 m/s.

2. INTRODUCTION

At GMT 2026-01-23, 023/18:13, the International Space Station (ISS) was to begin about an 26-minute reboost using the Dragon SpX-33 thrusters via its trunk kit. Figure 2 shows an artist's depiction of visiting vehicles' layout with the Dragon vehicle as it was docked with its thrusters pointed in the direction shown and thereby providing thrust along the velocity vector – a pre-maneuver was needed so that the ISS' "negative X direction" was aligned with the velocity vector at the time of the reboost. This arrangement brought the necessary orbital mechanics into play so as to speed up the ISS in its direction of "flight" (prograde), that is, along its velocity vector at that time – see vector annotations in Figure 2. This ultimately resulted in an altitude increase of about 4.34 km for the space station after this dynamic event. An intended ΔV metric of 2.405 m/s for the massive space station was predicted and comparing to estimates derived from SAMS measurements, this metric was 96% achieved.

3. QUALIFY

This section provides a mostly qualitative, figure-by-figure descriptive walk-through starting with the as-flown timeline shown on page 9.

Descriptive Walkthrough of Figures:

Figure 3, page 9: `As-Flown Timeline`
The as-flown timeline showing time hacks for salient events related to this Dragon Reboost objective: (1) maneuver to -XVV attitude, (2) settling burns + reboost, (3) maneuver back to nominal +XVV attitude.

Figure 4, page 10: `3D: Patterns, Structures, and Boundaries`
An 8-hour, 10 Hz spectrogram computed from measurements by the SAMS sensor head (121f05) in the JEM (JPM1F1) rack. This shows boundaries and patterns in 3 dimensions: time, vibratory frequency, and vibration magnitude. Annotations call attention to: (1) two crew exercise periods that come before the reboost activity, and (2) a black rectangular snippet that results in the inset figure showing 2 gross features of such a Dragon reboost. These 2 features also happen to show a fundamental characteristics of time vs. frequency characteristics. That is, “narrow in time implies wide in frequency” and “spread in time implies narrow in frequency”. The first gross feature is the settling burns over the span of ~3 minutes with a firing every 5 seconds or so. Each of these quick burst firings are narrow in time so they manifest as spread out in frequency, which we see as the vertical train/ladder of red spectral peaks before the actual reboost begins – this train/ladder of spectral peaks are odd harmonics of the main truss’ fundamental frequency. These are followed by the second gross feature, which is the reboost itself. The reboost is spread out over several minutes in time, so it manifests as narrow in frequency. The leftward pointing red arrow in the inset image shows that the reboost impact is mostly confined to the lowest frequency bin, a red horizontal streak at the bottom of the spectrogram, and the blue double-ended arrow shows the duration of the reboost event.

Fig. 5, Fig. 6, Fig. 7, pages 11-13: `30 Hz Spectrograms`
A trio of 6-hour, 30 Hz spectrogram computed from measurements by the SAMS sensor head (121f05) in the JEM (JPM1F1) rack, (121f02) on the Columbus module’s endcone, and (121f03) in the LAB (LAB1O1) rack, respectively. This affirms earlier assertions of *main truss fundamental and odd harmonics up to ~20 Hz* were excited with response throughout all 3 main labs of the ISS.

Figure 8, page 14: `The Leading Edge of Dragon Reboost`
The data in this figure was recorded by the SAMS (es20) sensor head mounted on the seat track of LAB1S2 (MSG). It serves to compare the light blue, as-measured (200 Hz) acceleration data versus time to the black, 6 Hz (low-pass filtered) data set. A rough cut suggests that the 200 Hz data "barely notices" the settling burns before the reboost begins, while the 6 Hz data set has this as the prominent feature leading into the reboost event itself, which is a step/plateau in the -X-axis direction for several minutes. Furthermore, the X-axis shows the highest peak-to-peak magnitudes, followed by the Y-axis, then the Z-axis. The Dragon’s thrusters were indeed aligned with the X-axis, albeit the Y-axis (we will see later) does some interesting alternating between port- and starboard-directed thrusts, seemingly to net balance out the settling in that direction.

Figure 9, page 15: `Dragon Settling Burns, Zoom-In (200 Hz)`
A short-duration (~12-second) plot of XYZ acceleration versus time, again using the SAMS data of sensor head es20 mounted on the MSG seat track. This gives us some keen insight despite being heavily ensconced in higher-frequency vibrations. With this time-zoom look, we can see settling burns #2 and #3 (from a total of 18 such thruster firings) with #2 being portward directed, then #3 being starboard directed. This back-and-forth pattern continues throughout the 3-minutes (18 firings in total) on the Y-axis. Note that the X-axis shows a short ringout for #2 and #3 and these firings are hardest to discern on the Z-axis.

Figure 10, page 16: `Dragon Settling Burns, Zoom-In & Overlay Insight`

With the exception of the vertical axis scaling, this figure is a repeat of the previous figure...albeit here with 200 Hz data shown as light blue traces overlayed with 6 Hz low-pass filtered data shown as the black traces. This gives way to important insight. We now clearly see structural ringout of the main truss on the ISS responding to the "hammer hits" of the Dragon’s thrusters.

We see those last a few seconds, but those are left to dampen/die out naturally on their own before the next settling burn thruster firing ("hammer hit") is initiated. This is an important consideration as ill-timed thruster firings could amplify main truss vibrations and thereby unnecessarily subject the structure to undesirable, extra load cycles. We saw earlier in the color spectrogram the train of spectral peaks (harmonics) of the main truss vibrational response to the "hammer hit" stimulus, and here we see those were mainly X-axis aligned accelerations of the largest, single structure on the ISS, the main truss.

Figure 16, page 20: `Dragon Tank Swap`
This figure has dimmed/gray annotations addressed in the next section, however, we point out here that on occasion a "tank swap" can sometimes occur during such a Dragon reboost and that is the pink annotations in this figure.

Fig. 18 & Fig. 19, page 21: `Two Optimized Propellant Maneuvers`
These 2 figures show (on the left side of page): an estimate of the quasi-steady acceleration data throughout the reboost activities bracketed on either end by 2 Optimized Propellant Maneuvers (OPMs), and (on the right side of the page): the yaw, pitch, and roll angles of the ISS during this same span. These angular data may be better for visualizing, e.g. buoyancy effects.

4. QUANTIFY

To complement the mostly qualitative look at the acceleration measurements in the previous section, we now quantify the microgravity environment impact of the Dragon reboost event across multiple SAMS sensor heads in the three main ISS laboratories using three explicit metrics: (1) mean X-axis acceleration during the reboost event, (2) duration of the negative X-axis step, and (3) the resultant, computed ΔV value.

We see a consistent accounting of these metrics from seven SAMS sensor heads that were active during this Dragon reboost – starting with Figure 11 on page 17 and going on through Figure 17 on page 20. Although, we note here that the annotations on the last 2 figures are dimmed/grayed out since our signal feature extraction routine was tripped up by the settling burns in those 2 data sets. For questions or such regarding methods used herein (i.e. signal processing chain), then send an email to pimsops@lists.nasa.gov with details of your inquiry...in the meanwhile, see Appendix A for some of the technical details.

A quantification of the reboost impact measured by the distributed SAMS sensors is provided in Table 1 below, and the key values can be visualized from plots in Figure 11 through Figure 17. These seven SAMS sensor heads recorded the reboost and related events independently, while utilizing a common time base synchronized via an ISS NTP time server.

Table 1. Metrics based on -X-axis steps from 5 of 7 SAMS sensors.

Sensor	|X-Axis| (mg)	Duration (mm:ss)	ΔV (m/s)	Location
121f03	0.169	23:09	2.31	LAB1O1 (ER2)
es18	0.171	23:07	2.33	LAB1O4 (ER6)
121f02	0.169	23:09	2.30	COL Endcone
121f08	0.169	23:09	2.30	COL1A3 (EPM)
es19	0.171	23:07	2.32	JPM1F1 (ER4)
es20	—	—	—	LAB1S2 (MSG)
121f05	—	—	—	JPM1F1 (ER5)

5. METHODS

Method for Estimating ΔV From SAMS Measurements

SAMS accelerometer measurements were processed per sensor to estimate the vehicle reboost ΔV along the velocity vector's direction. In brief, we knew a priori that the ISS would be maneuvered such that the velocity vector during the reboost span would be aligned with the -X-axis for all of the SAMS sensor heads, so $a_{vv}[k]$ in this discussion would simply be the negative of the SAMS X-axis data for the reboost event.

As a result, $a_{vv}[k]$ was run through a *mostly* robust, sliding, piecewise-constant (PWC) median filter (kernel size = 33 samples) in order to suppress high-frequency fluctuations while preserving steep step transitions; and thus preserve step timing. These steps at time (t_1, t_2) were henceforth detected by correlating the PWC-filtered series with a discrete edge kernel (a first-difference template $[-1, 0, 1]$) and selecting the indices of maximum and minimum correlation as the leading and trailing edges of the reboost step, respectively.

With (t_1,t_2) established, ΔV was computed from the PWC filter's input of 5-second interval averaged X-axis acceleration data using a *rectangular (plateau) approximation*: the mean acceleration over the plateau window multiplied by the plateau duration. That is, $\Delta V \approx \bar{a}_{vv}\,(t_2 - t_1)$, where $\bar{a}_{vv}$ is the arithmetic mean of $a_{vv}[k]$ over the sample indices $[k_1,k_2]$ corresponding to the time span $[t_1,t_2]$. For those interested, Appendix A gives better implementation notes.

Method for Estimating Δh From SAMS Measurements

This method relied heavily on the references shown after Appendix C. In short, the estimated, velocity-vector-aligned ΔV from SAMS provides a first-order approximation for the maneuver's small prograde velocity increment Δv. Assuming a near-circular orbit, the corresponding altitude gain Δh can be approximated from Δv using standard orbital-energy relationships (equivalently, the *vis-viva equation*). In this report, Δh is computed from the measured $\Delta v \approx \Delta V$ using the first-order relation derived in Appendix B, with the supporting energy-form identity shown in Appendix C.

6. CONCLUSION

The SpaceX Dragon SpX-33 reboost on GMT 2026-01-23 demonstrated the Dragon vehicle's capability to increase the orbital altitude of the ISS. According to the as-flown timeline and data from distributed SAMS sensors, the reboost followed a structured sequence: an initial -XVV attitude maneuver, a ~3-minute series of settling burns, a sustained ~23-minute thrust phase, and a concluding +XVV attitude maneuver.

The vibratory environment was dominated by 18 settling burn pulses during the ~3-minute span. These 'hammer hits,' spaced at approximately 5-second intervals, excited global structural modes—most notably the 0.1 Hz main truss resonance. This resulted in a distinctive harmonic train visible up to ~20 Hz across all SAMS spectrograms, driven by the main truss's response to these impulsive stimuli.

Quantitative Summary

- **Delta-V:** Estimates computed from SAMS measurements suggested a ΔV of ~2.31 m/s, reaching 96% of the flight controller's 2.405 m/s prediction.
- **Acceleration Magnitude:** A steady-state negative X-axis plateau of roughly -0.17 mg was maintained throughout the primary reboost window.
- **Main Events:** The main events comprised a ~3-minute settling burn sequence followed by ~23 minutes and 8 seconds of continuous thruster firing to nearly achieve the desired velocity change over that span. These were book-ended by maneuvers, first "to -XVV", then "back to +XVV" attitude.
- **Orbital Result:** The reboost ultimately resulted in an ISS altitude increase of 4.34 km – reported by flight controllers, whereas the first-order approximation based on SAMS measurements suggested an increase of 4.05 km.

Operational Insights

- While the five-second intervals between settling burns triggered significant vibratory disturbances across the ISS, the timing was engineered with the precision of ancient Incan masonry. Just as their stones fit together so tightly as to leave no room for mortar, these pulses were spaced to allow for natural structural ringout—preventing the 'mortar' of constructive interference from amplifying truss vibration loads and ensuring sound structural housekeeping.
- The environmental impact of a reboost is not limited to the firing window but includes the broader spans of RS attitude control, large-scale attitude maneuvers, and settling burns when the Dragon is used.
- SAMS continues to provide a vital "truth" source for validating flight predictions and characterizing the impact of visiting vehicle thrusters on the ISS microgravity environment.

APPENDIX A
METHOD FOR ESTIMATING ΔV FROM SAMS MEASUREMENTS

This appendix documents the procedure used to estimate the velocity-vector-aligned ΔV attributable to the reboost-induced step observed in the SAMS accelerometer measurements.

A. Discrete-time definitions and projection

Let $\mathbf{a}[k]$ denote the triaxial accelerometer measurement at sample index k, sampled at rate F_s (samples/s) on a uniform grid $t[k] = t_0 + k/F_s$. Let $\hat{\mathbf{u}}_{vv}$ denote the along–velocity-vector unit direction over the event epoch. The scalar component of interest was simply X-axis data:

$$a_{vv}[k] \;=\; \mathbf{a}[k] \cdot \hat{\mathbf{u}}_{vv}. \tag{1}$$

B. Denoising and step-edge detection

The step edge indices are determined from a denoised version of the X-axis acceleration data to improve robustness in the presence of vibratory content:

- The normalized velocity-vector component was denoised using a sliding piecewise-constant (PWC) median filter (kernel size of 33 samples) to suppress high-frequency fluctuations while preserving step transitions.
- Step timing was then detected by correlating the filtered velocity-vector component with a discrete edge kernel (a first-difference template $[-1,0,1]$) and selecting the indices of maximum and minimum correlation as the rising and falling step edges, respectively.

In practice, correlation with $[-1,0,1]$ is equivalent to applying a short, discrete derivative-like operator to the filtered sequence; selecting the extreme correlation indices provides a simple and effective way to localize step edges in the presence of residual noise.

C. Plateau window and statistics

Let k_1 and k_2 be the detected rising and falling edge indices for a sustained step (with $k_1 < k_2$), and let $t_1 = t[k_1]$ and $t_2 = t[k_2]$ be the corresponding times. The plateau duration is

$$\Delta t \;=\; t_2 - t_1 \;=\; \frac{k_2 - k_1}{F_s}. \tag{2}$$

Over this interval, we compute a plateau mean of the *pre-PWC-filtered* 5-second interval averaged X-axis acceleration:

$$\bar{a}_{vv} \;=\; \frac{1}{N} \sum_{k=k_1}^{k_2-1} a_{vv}[k], \qquad N \;=\; k_2 - k_1. \tag{3}$$

(Using the unfiltered $a_{vv}[k]$ for the mean avoids biasing the amplitude estimate by the denoiser; the denoised series was used only to improve edge timing.)

D. Computing ΔV from discrete-time data

The continuous-time identity $\Delta V = \int a_{vv}(t)\,dt$ can be considered here, but only as a conceptual reference. In this work, ΔV is computed from discrete-time SAMS data using a *rectangular (plateau) approximation* based on the detected window $[t_1, t_2]$:

$$\Delta V \;\approx\; \bar{a}_{vv}\,\Delta t, \tag{4}$$

where $\bar{a}_{vv}$ is the plateau mean defined above and $\Delta t = t_2 - t_1$. Importantly, we do *not* perform a sample-by-sample numerical integration of $a_{vv}[k]$; instead, the estimate is "plateau mean times duration," which is appropriate for our plateau signal feature extraction where the dominant structure is well represented by a mean level over a duration. As such, we effectively ignored brief excursions like the tank swap during the reboost plateau.

E. Units conversion

When $a_{vv}[k]$ is expressed in μg, the conversion to $\mathrm{m/s^2}$ uses $g_0 = 9.81\,\mathrm{m/s^2}$:

$$a_{vv}\;[\mathrm{m/s^2}] \;=\; a_{vv}\;[\mu g] \times 10^{-6} \times g_0. \tag{5}$$

With a_{vv} in $\mathrm{m/s^2}$ and Δt in seconds, ΔV follows directly from $\Delta V \approx \bar{a}_{vv}\,\Delta t$. We used plots to show these features and extracted metrics for all seven SAMS sensors active during the reboost and notably 2 sensor heads' data tripped up our automated feature extraction using the methodology described here.

APPENDIX B
APPROXIMATE ALTITUDE GAIN FROM A SMALL PROGRADE Δv

A quick, first-order way to estimate the altitude gain from a reboost is to relate a small *prograde* (along-track) velocity increment Δv to the corresponding change

in orbital energy and semi-major axis. For a near-circular orbit, the altitude is approximately $h \approx a - R_E$, so a small change in semi-major axis Δa is a good proxy for altitude change Δh:

$$\Delta h \approx \Delta a \qquad \text{(near-circular orbit approximation)}. \tag{6}$$

A. Derivation (first order)

The specific orbital (mechanical) energy is

$$\epsilon = \frac{v^2}{2} - \frac{\mu}{r} = -\frac{\mu}{2a}, \tag{7}$$

where μ is Earth's gravitational parameter, r is orbital radius, v is orbital speed, and a is the semi-major axis [4], [5].

For a small prograde increment Δv, the leading-order change in specific energy is obtained by expanding the kinetic-energy term:

$$\Delta\left(\frac{v^2}{2}\right) = \frac{(v+\Delta v)^2 - v^2}{2} = v\,\Delta v + \frac{(\Delta v)^2}{2}. \tag{8}$$

Retaining only the linear term (and neglecting the quadratic correction) gives the first-order approximation

$$\Delta\epsilon \approx v\,\Delta v. \tag{9}$$

The ratio of the neglected term to the retained term is

$$\frac{\frac{(\Delta v)^2}{2}}{v\,\Delta v} = \frac{\Delta v}{2v}, \tag{10}$$

which is $\Delta v/v \ll 1$ when $\Delta v \ll v$. For this Dragon reboost, we computed $\Delta v \approx 2$ m/s, with $v \approx 7.7\times10^3$ m/s showing that the velocity was nearly 4 orders of magnitude greater than the Δv increment.

Differentiating the energy form $\epsilon = -\mu/(2a)$ yields

$$\Delta\epsilon = \frac{\mu}{2a^2}\,\Delta a. \tag{11}$$

Equating Eqs. (9) and (11) gives

$$\boxed{\Delta a \approx \frac{2a}{v}\,\Delta v} \quad \Rightarrow \quad \boxed{\Delta h \approx \frac{2a}{v}\,\Delta v}. \tag{12}$$

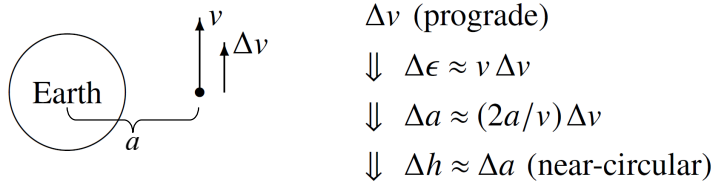

Fig. 1: Conceptual sketch & 1st order chain to link small prograde Δv to approx. altitude gain, Δh, for near-circular orbit (*not to scale*).

B. Representative ISS orbit parameters

For an ISS-like, near-circular orbit, a representative semi-major axis is

$$a \approx R_E + h, \tag{13}$$

where $R_E \approx 6371\,\text{km}$ and a typical ISS altitude is on the order of $h \sim 400\,\text{km}$ [3], [1], [2]. This yields

$$a \approx 6371\,\text{km} + 400\,\text{km} = 6771\,\text{km}. \tag{14}$$

A representative orbital speed is $v \sim 7.7\,\text{km/s}$ [1], [3], [2].

C. Example (consistency check)

Using $a = 6771\,\text{km}$, $v = 7.7\,\text{km/s}$, and a reboost magnitude $\Delta v = 2.3\,\text{m/s} = 2.3\times10^{-3}\,\text{km/s}$, Eq. (12) gives

$$\Delta h \approx \frac{2(6771\,\text{km})}{7.7\,\text{km/s}}\left(2.3\times10^{-3}\,\text{km/s}\right) \approx 4.05\,\text{km}, \tag{15}$$

which is consistent (to first order) with the reported altitude gains for reboost events of this magnitude.

APPENDIX C
ENERGY-FORM IDENTITY USING THE VIS-VIVA EQUATION

This appendix shows the algebraic steps that connect the middle and rightmost forms of the specific orbital energy equation in Eq. (7). The key bridge is the vis-viva equation, valid for Keplerian two-body motion (all conic sections) [4], [5]:

$$v^2 = \mu\left(\frac{2}{r} - \frac{1}{a}\right). \tag{16}$$

Divide Eq. (16) by 2:

$$\frac{v^2}{2} = \frac{\mu}{2}\left(\frac{2}{r} - \frac{1}{a}\right). \tag{17}$$

Distribute the factor $\mu/2$:

$$\frac{v^2}{2} = \mu\left(\frac{1}{r}\right) - \frac{\mu}{2a}. \tag{18}$$

Substitute Eq. (18) into the definition $\epsilon = v^2/2 - \mu/r$:

$$\epsilon = \left(\mu\frac{1}{r} - \frac{\mu}{2a}\right) - \frac{\mu}{r} \tag{19}$$

$$= \mu\frac{1}{r} - \frac{\mu}{2a} - \frac{\mu}{r} \tag{20}$$

$$= -\frac{\mu}{2a}. \tag{21}$$

REFERENCES

[1] European Space Agency (ESA), "ISS: International Space Station" (web page), includes on-orbit altitude and velocity ranges. Accessed Jan. 28, 2026. https://www.esa.int/Science_Exploration/Human_and_Robotic_Exploration/International_Space_Station/ISS_International_Space_Station

[2] NASA, "International Space Station Reference Guide" (PDF), Nov. 2010, includes altitude range and orbital speed. Accessed Jan. 28, 2026. https://www.nasa.gov/wp-content/uploads/2022/06/508318main_iss_ref_guide_nov2010.pdf

[3] NASA, "STEMonstrations: Classroom Connections – Orbits" (PDF), includes representative ISS altitude and speed. Accessed Jan. 28, 2026. https://www.nasa.gov/wp-content/uploads/2018/06/stemonstrations_orbits.pdf

[4] A. V. Rao, "Orbital Mechanics: An Introduction" (course notes, PDF), includes specific energy and vis-viva relationships. Accessed Jan. 28, 2026. https://www.anilvrao.com/resources/EAS4510-Course-Notes.pdf

[5] R. F. Stengel, "Orbital Mechanics" (MAE 342 Lecture Notes, PDF), includes vis-viva / energy-integral forms. Accessed Jan. 28, 2026. https://stengel.mycpanel.princeton.edu/MAE342Lecture2.pdf

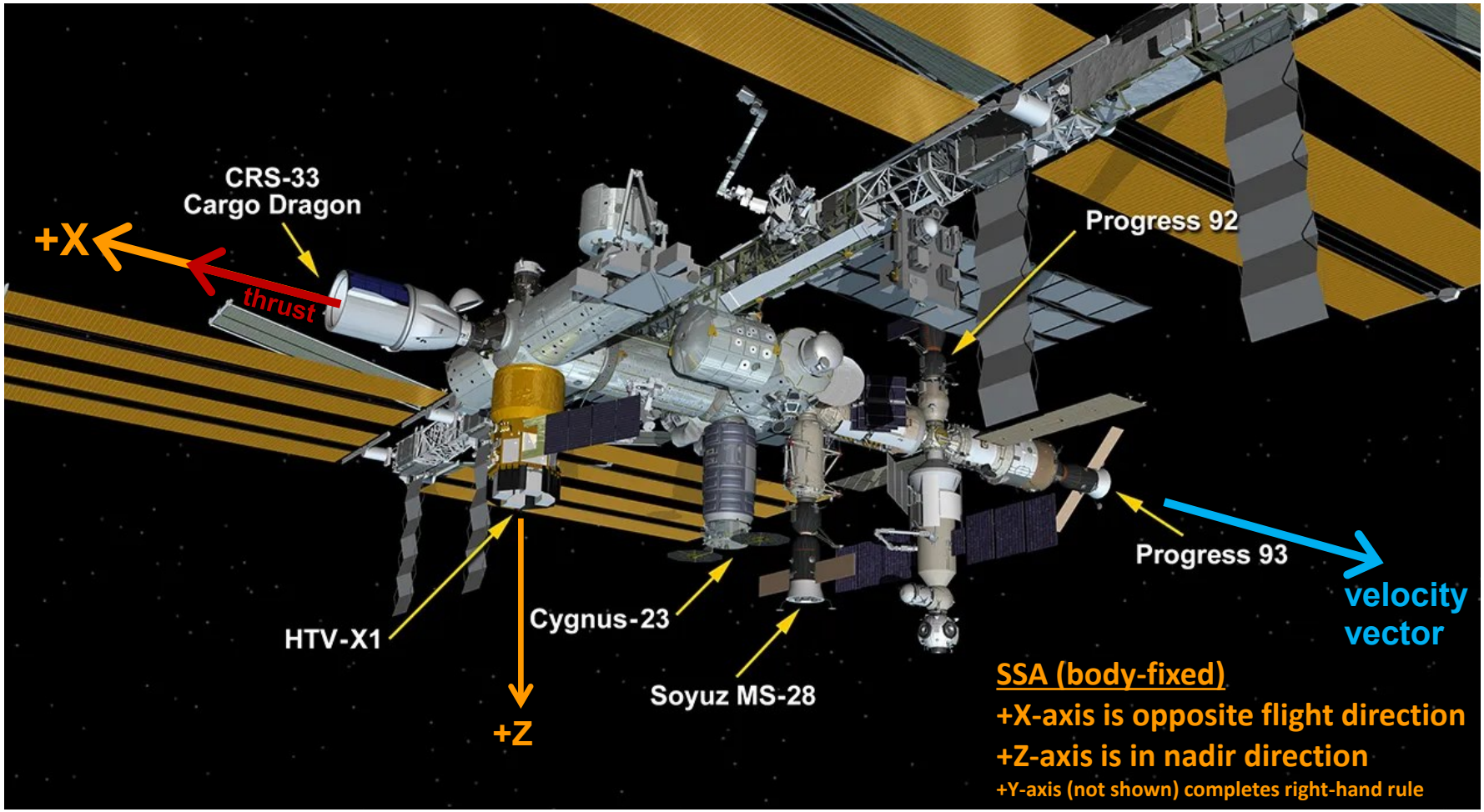

Fig. 2: SpX-33 Dragon's Location and Alignment during Reboost.

OPM to nXVV with Timeliner Profile 7 (M26_023_A_03.UAF)									**01/23/2026**
43	023/04:56:00 — 	Y	-18	+XVV +ZLV TEA	LVLH	356 356.7 0.9	MMT UST 	Transition to USTO	
44	023/04:56:01 023/06:27:40 	Y	-18	-XVV +ZLV 	LVLH	176 357.44 0.85	UST UST 	Mnvr to -XVV using OPM	Not a pure Eigen axis rotation - reference chit 19640 for attitude profile; One Rev Late Maneuver 023/06:29 - 023/08:01
45	023/06:51:00 — 	Y	-19	-XVV +ZLV 	LVLH	176 357.44 0.85	UST MMT 	Transition to Momentum Management using USTO	OPM Ending Attitude
46	023/06:51:01 023/06:56:00 	Y	-19	-XVV +ZLV TEA	LVLH	176 357.1 0.9	MMT MMT 	Mnvr to TEA on Momentum Management	Maneuver rate 0.001 deg/s; TEA for VV#1z N1nCN2nHzefD, PSARJ Auto, SSARJ Auto; Post-OPM thermal dwell 023/06:28-023/15:28
SpX-33 Dragon Reboost (M26_023_B_06.UAF)									**01/23/2026**
47	023/18:06:00 — 	Y	-21	-XVV +ZLV TEA	LVLH	176 357.1 0.9	MMT THR 	Handover US to RS	
48	023/18:07:00 023/18:12:00 	Y	-21	-XVV +ZLV TEA	LVLH	176 357.1 0.9	THR THR 	Quaternion update for reboost in TEA (Dragn2 on N2 Forward)	Settling burns beginning at 18:35:00, TIG 18:38:00 DUR 22:56
49	023/19:01:00 023/19:06:00 	Y	-21	-XVV +ZLV TEA	LVLH	176 357.1 0.9	THR THR 	Quaternion Update	
50	023/19:23:00 — 	Y	-21	-XVV +ZLV TEA	LVLH	176 357.1 0.9	THR MMT 	Handover RS to US Momentum Management	TEA for VV#1z N1nCN2nHzefD, PSARJ Auto, SSARJ Auto
OPM to pXVV with Timeliner Profile 15 (M26_023_C_03.UAF)									**01/23/2026**
51	023/23:32:00 — 	Y	-22	-XVV +ZLV TEA	LVLH	176 357.1 0.9	MMT UST 	Transition to USTO	
52	023/23:32:01 024/01:03:40 	Y	-22	+XVV +ZLV 	LVLH	356 357.1 0.85	UST UST 	Mnvr to +XVV using OPM	Not a pure Eigen axis rotation - reference chit 19640 for attitude profile; One Rev Late Maneuver 024/01:05 - 024/02:36
53	024/01:16:00 — 	Y	-22	+XVV +ZLV 	LVLH	356 357.1 0.85	UST MMT 	Transition to Momentum Management using USTO	OPM Ending Attitude
54	024/01:16:01 024/01:33:00 	Y	-22	+XVV +ZLV TEA	LVLH	356 356.7 0.9	MMT MMT 	Mnvr to TEA on Momentum Management	Maneuver rate 0.001 deg/s; TEA for VV#1z N1nCN2nHzefD, PSARJ Auto, SSARJ Auto; Post-OPM thermal dwell 024/01:04-024/10:04

Fig. 3: As-Flown Timeline: Maneuver to -XVV > Reboost > Maneuver Back to +XVV.

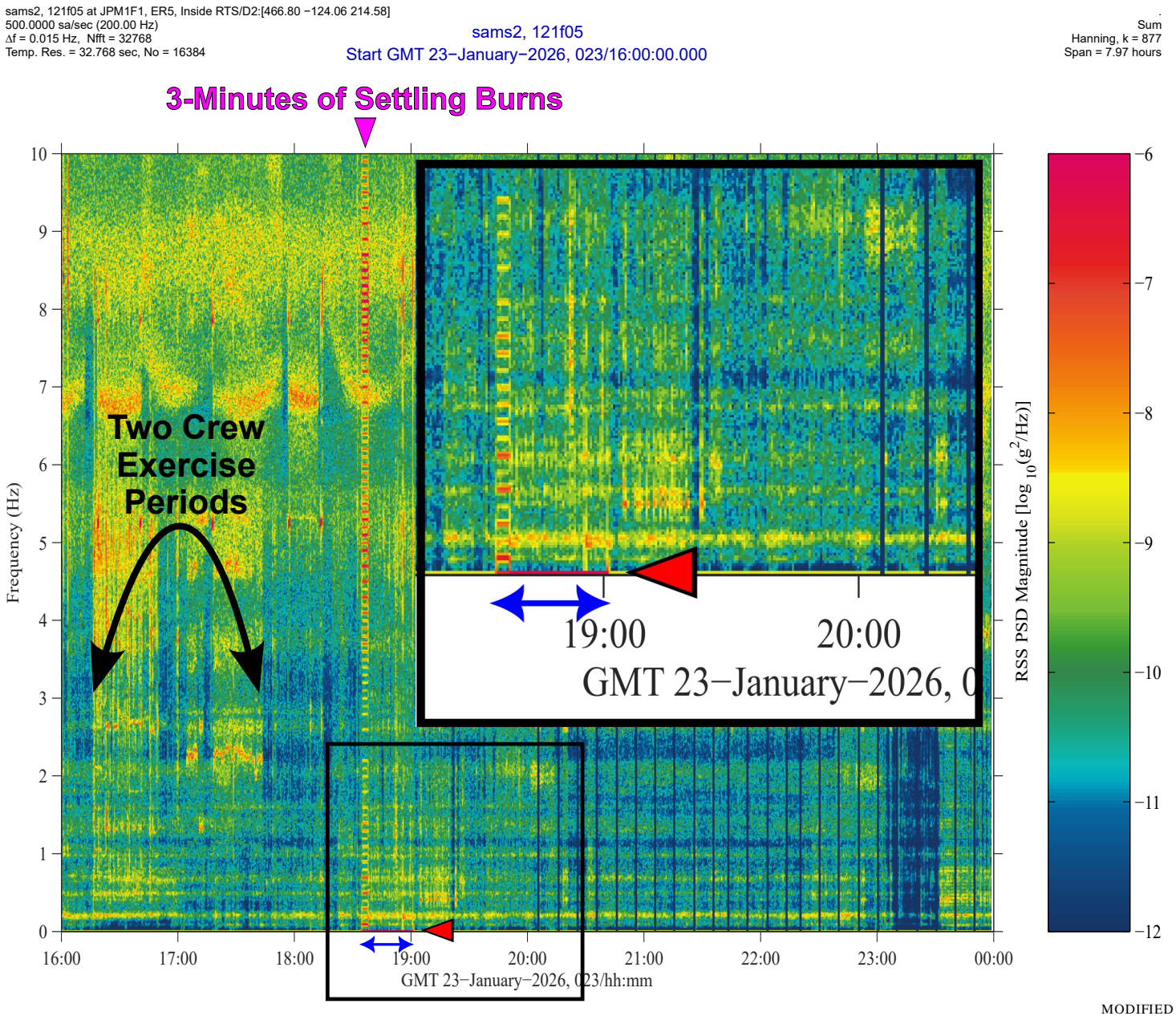

Fig. 4: 10 Hz Spectrogram showing Dragon SpX-33 Reboost on GMT 2026-01-23 from SAMS Sensor in the JEM on JPM1F1 Rack.

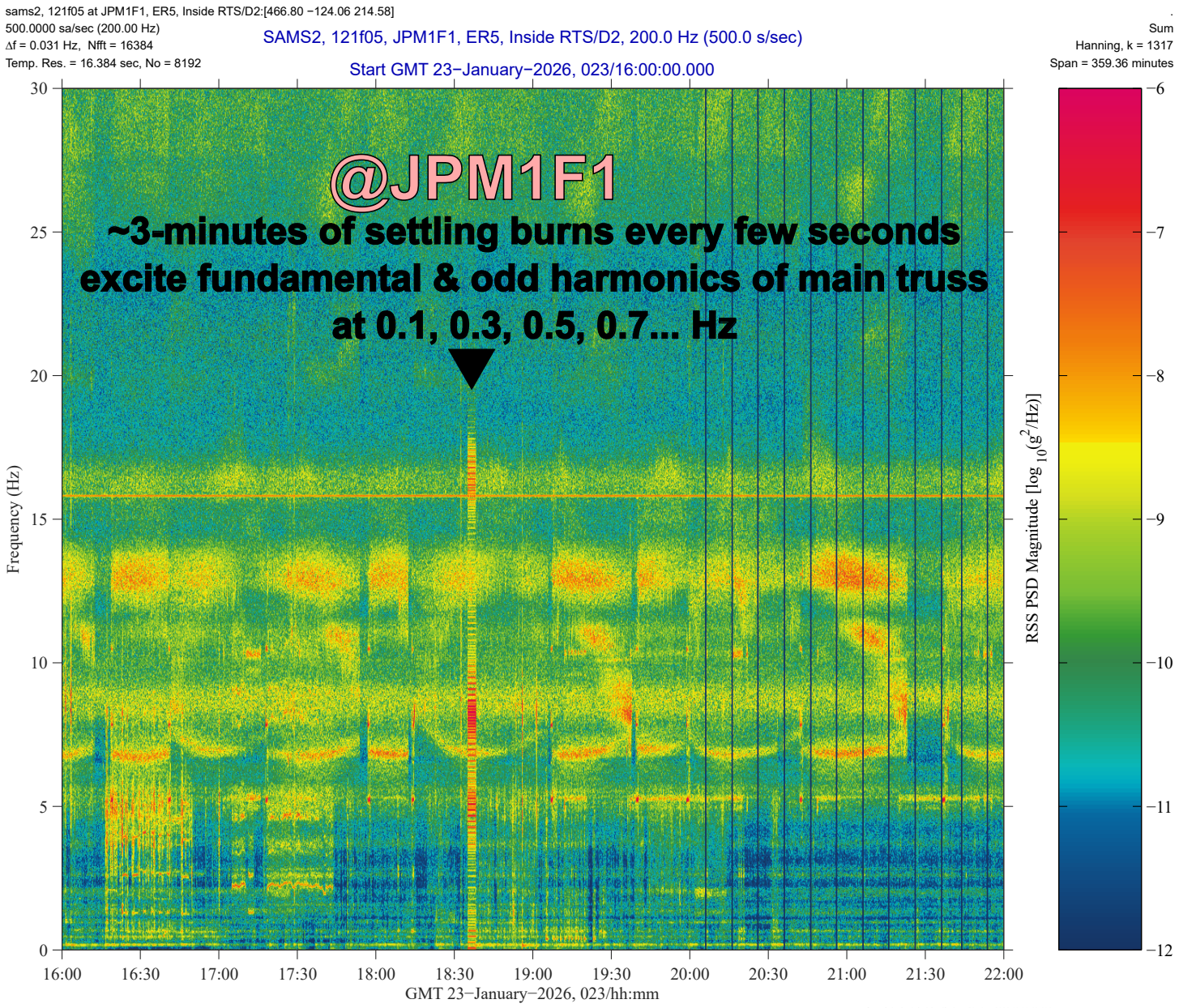

Fig. 5: 30 Hz Spectrogram showing Settling Burns Odd Harmonics Start at 0.1 Hz & Up to ~ 20 Hz SAMS Sensor on JPM1F1 Rack.

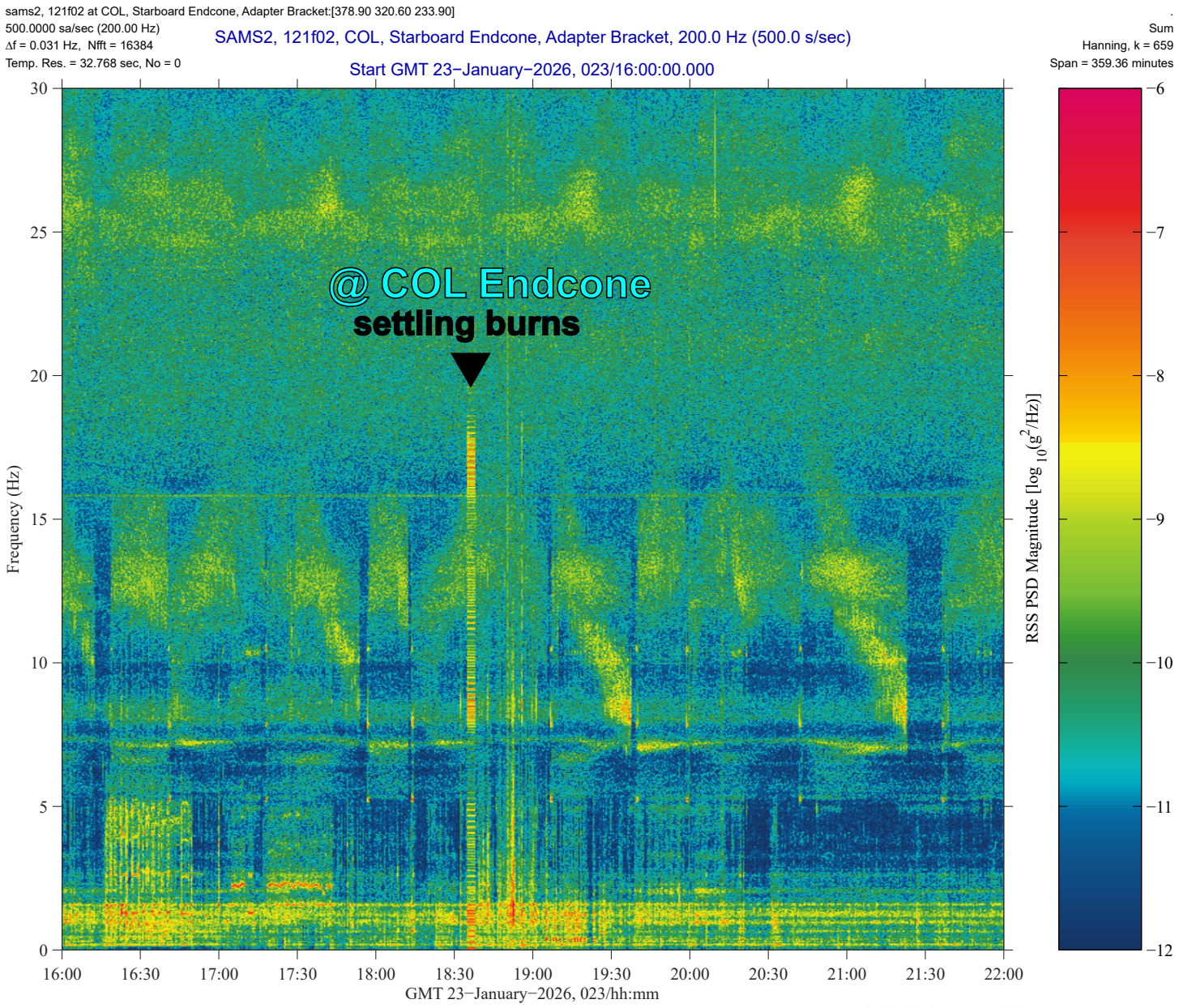

Fig. 6: 30 Hz Spectrogram showing Settling Burns Odd Harmonics Start at 0.1 Hz & Up to ~ 20 Hz SAMS Sensor on COL Endcone.

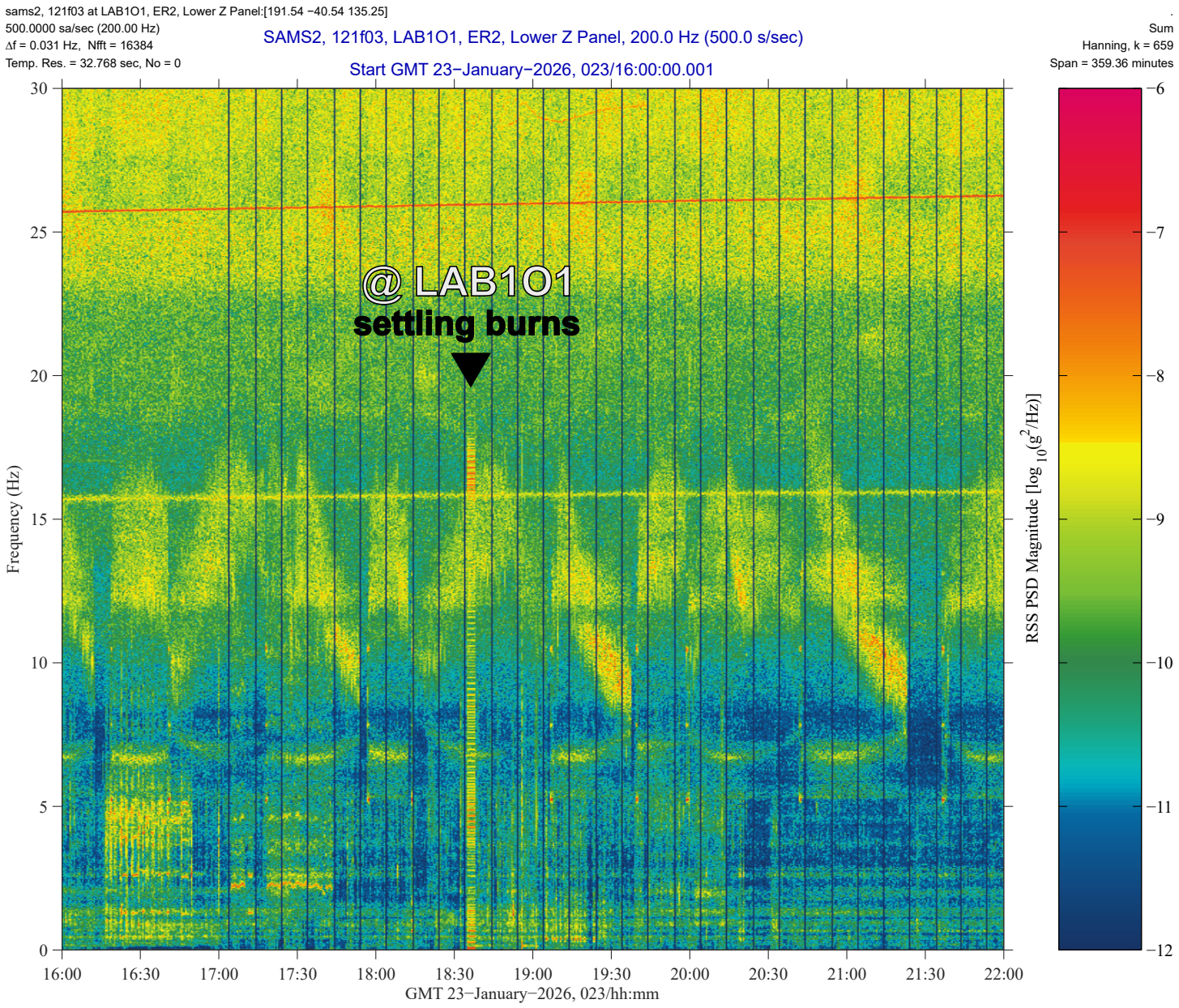

Fig. 7: 30 Hz Spectrogram showing Settling Burns Odd Harmonics Start at 0.1 Hz & Up to ~ 20 Hz SAMS Sensor on LAB1O1 Rack.

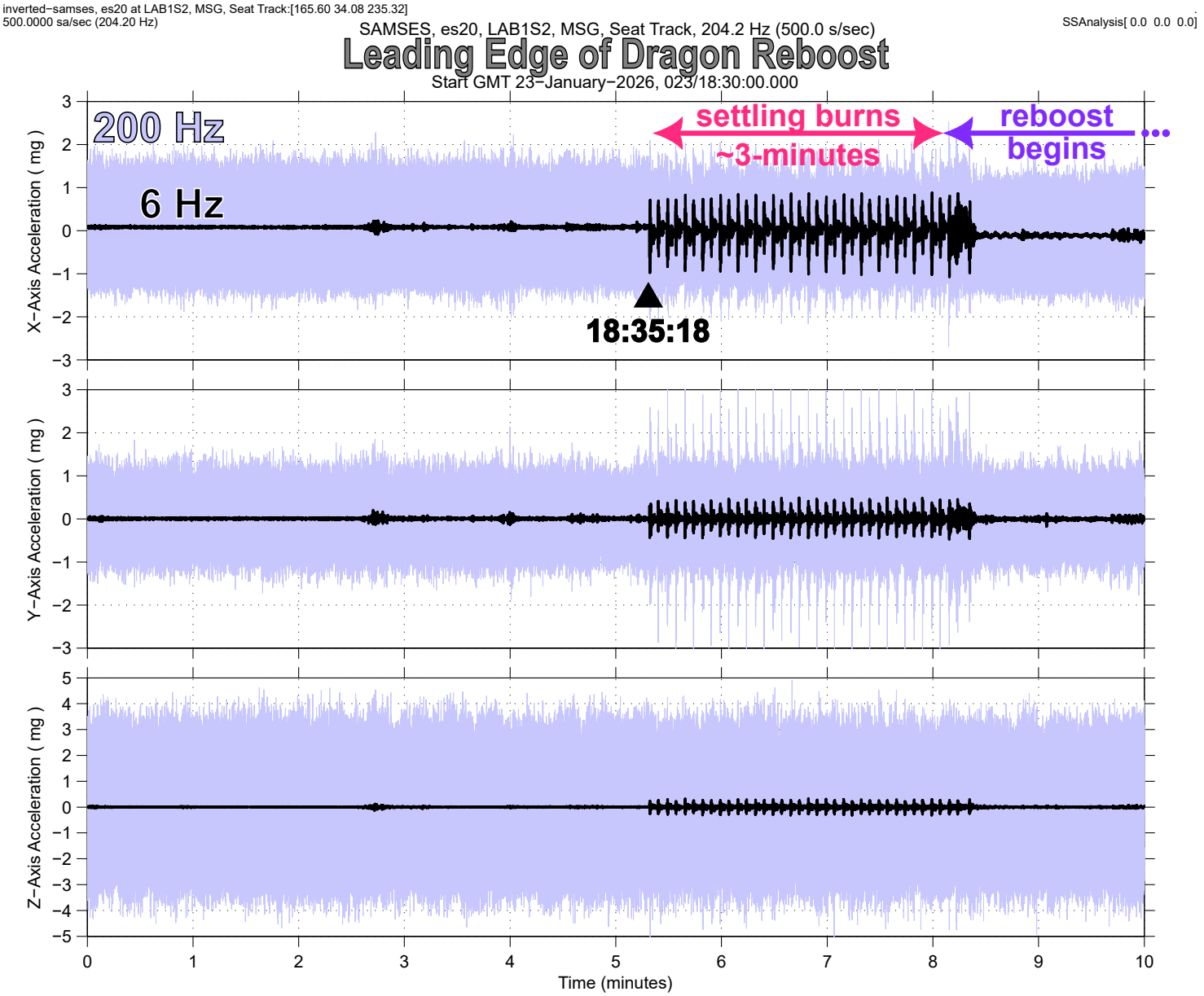

Fig. 8: 10-Minute Overlay Black=6 Hz on Blue=200 Hz $a(t)$ Leading Up to Settling Burns (es20 on MSG).

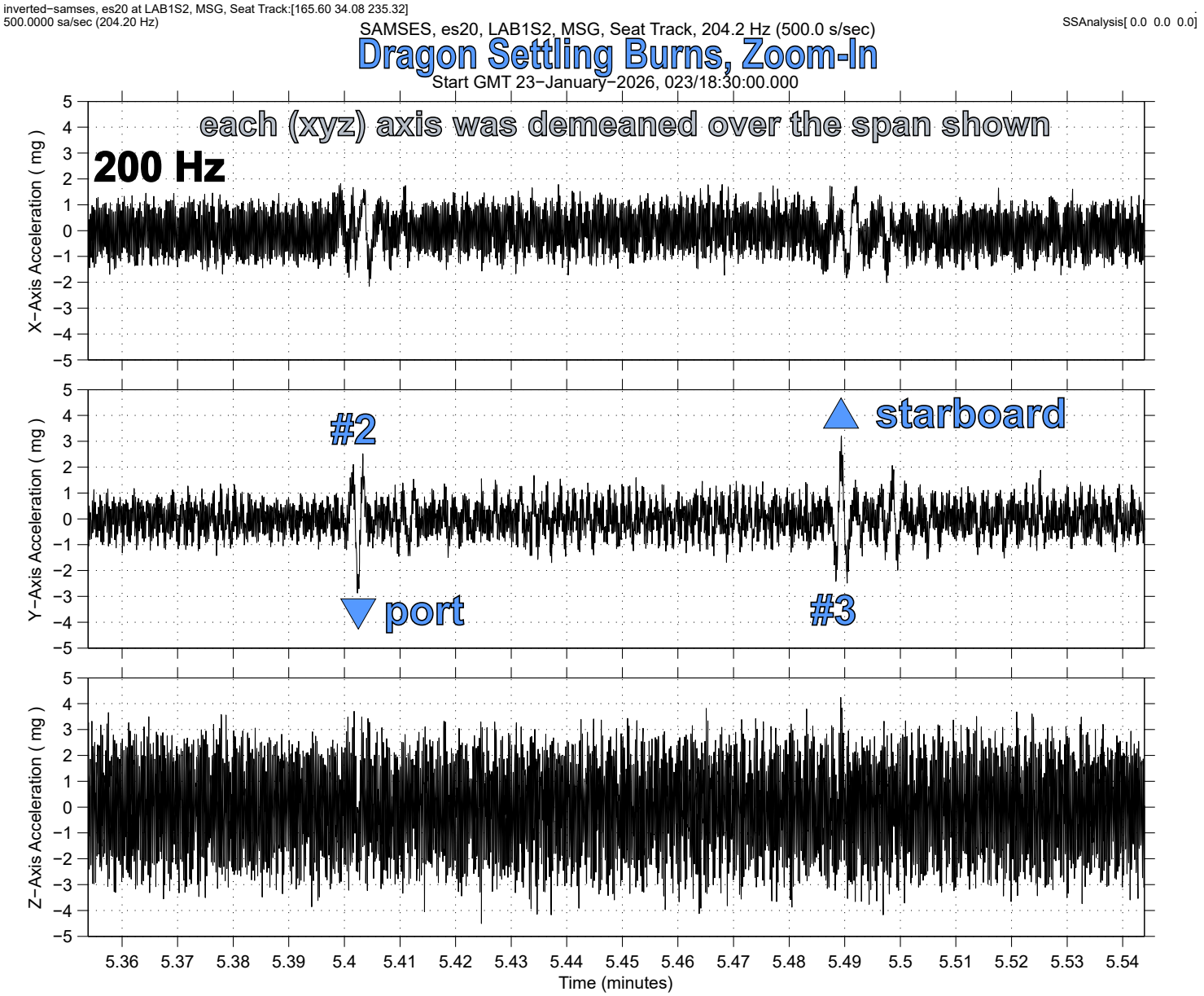

Fig. 9: 12-Second, 200 Hz $a(t)$ Showing 2 of 18 Settling Burn Thruster Firings (es20 on MSG).

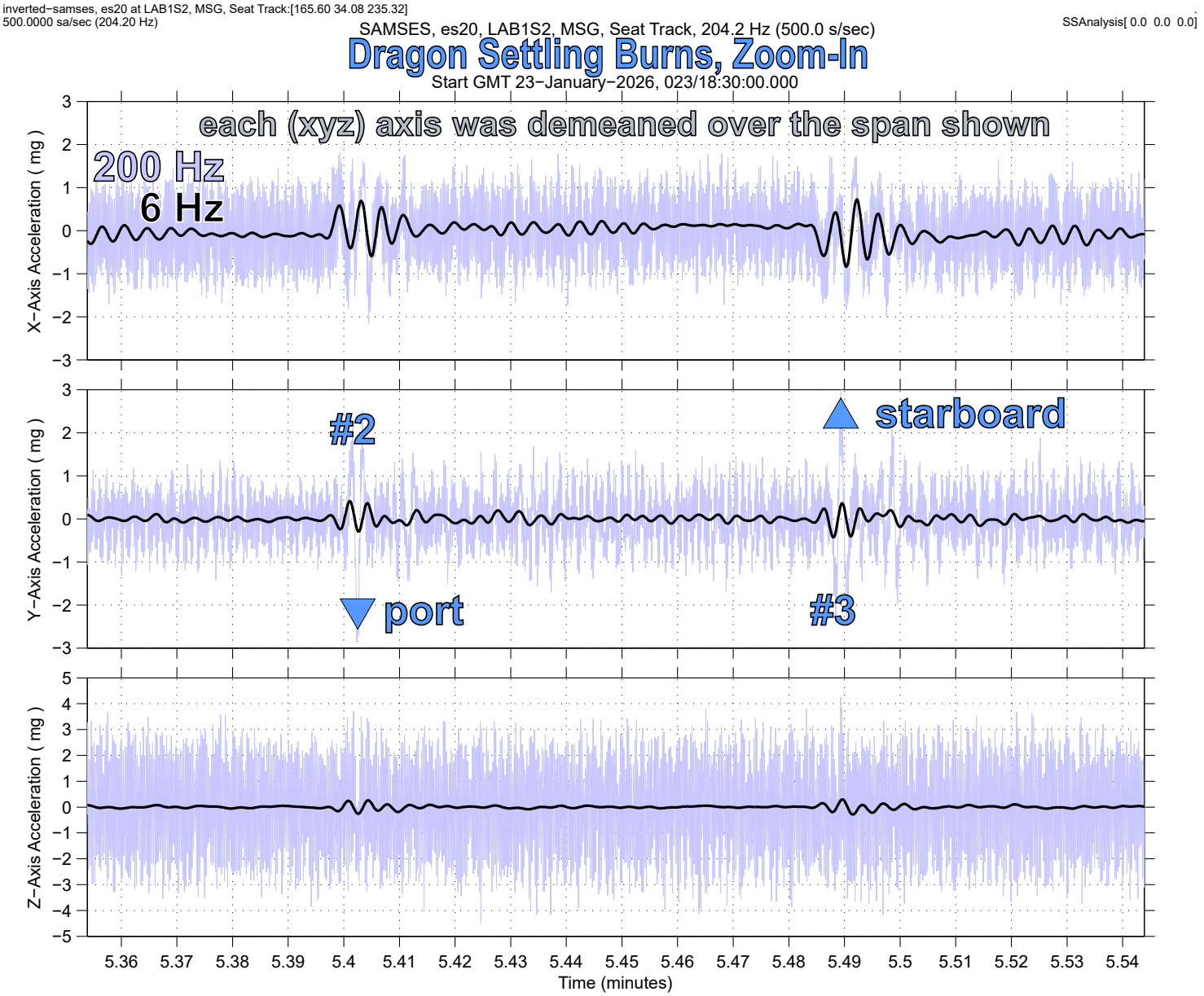

Fig. 10: Accel. vs. Time (Overlay 6 Hz low-pass filtered on 200 Hz) Showing 2 of 18 Settling Burn Thruster Firings (es20 on MSG).

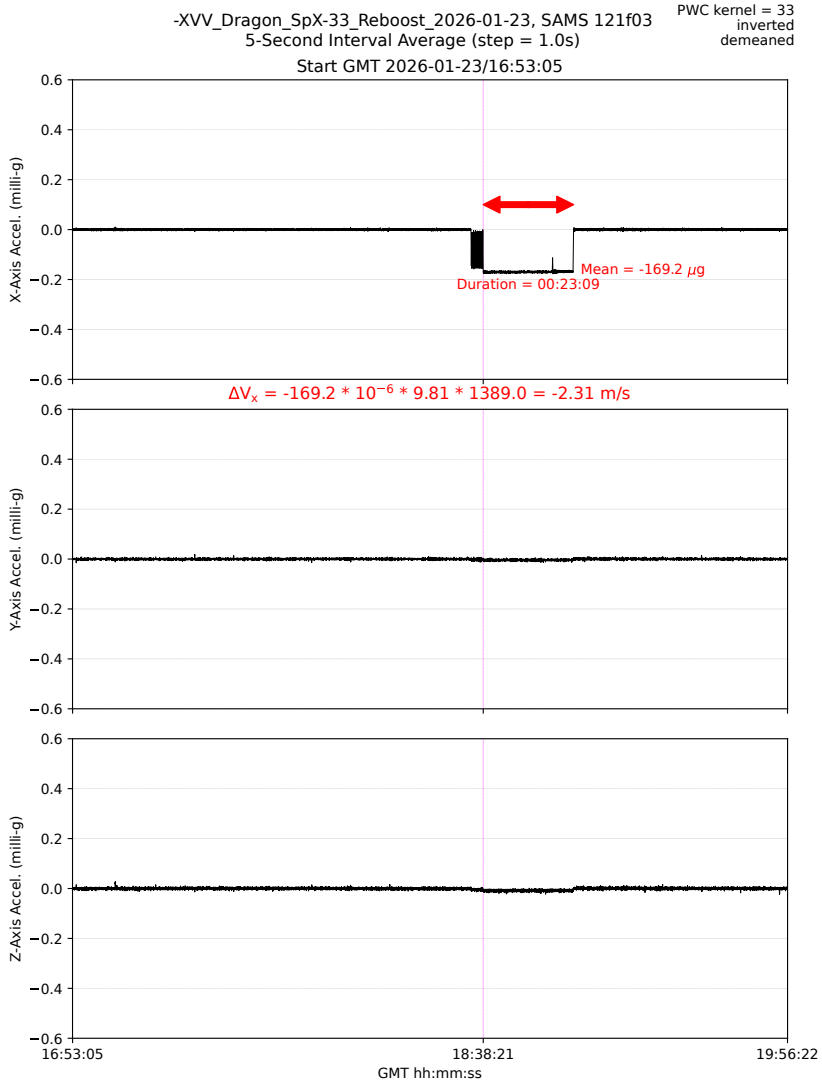

Fig. 11: 5-sec interval average for SAMS 121f03 sensor at LAB1O1 (ER2).

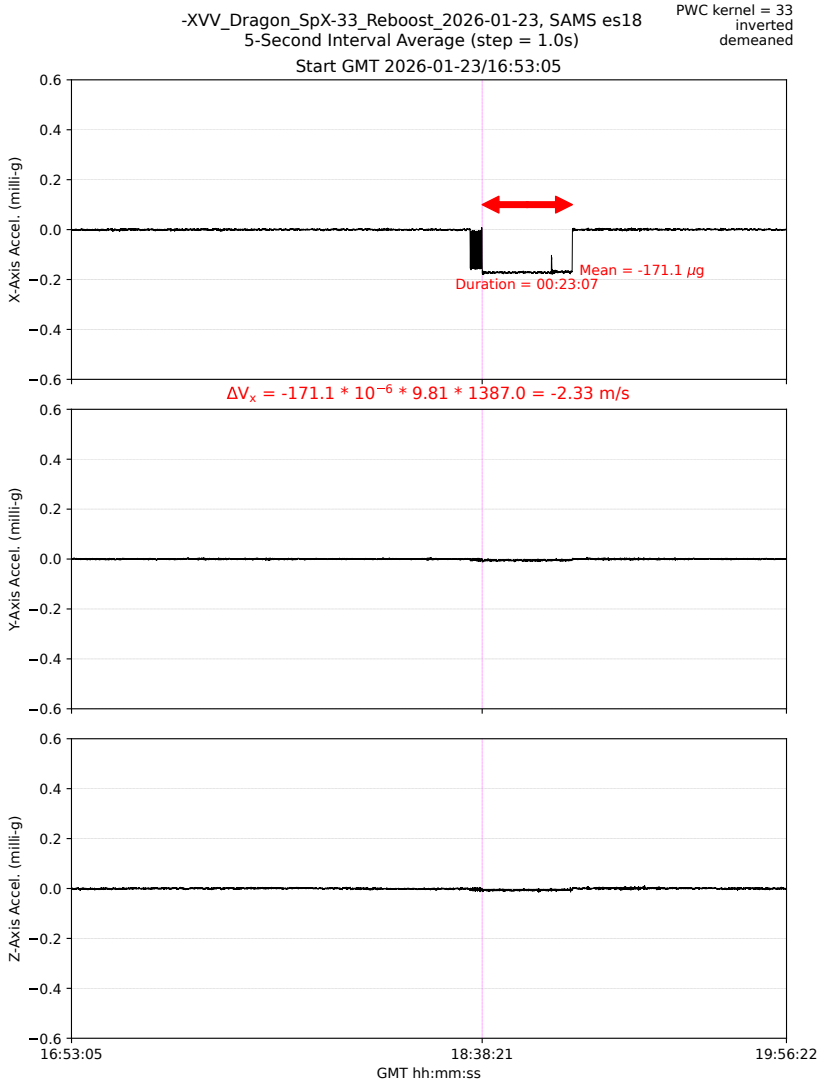

Fig. 12: 5-sec interval average for SAMS es18 sensor at LAB1O4 (ER6).

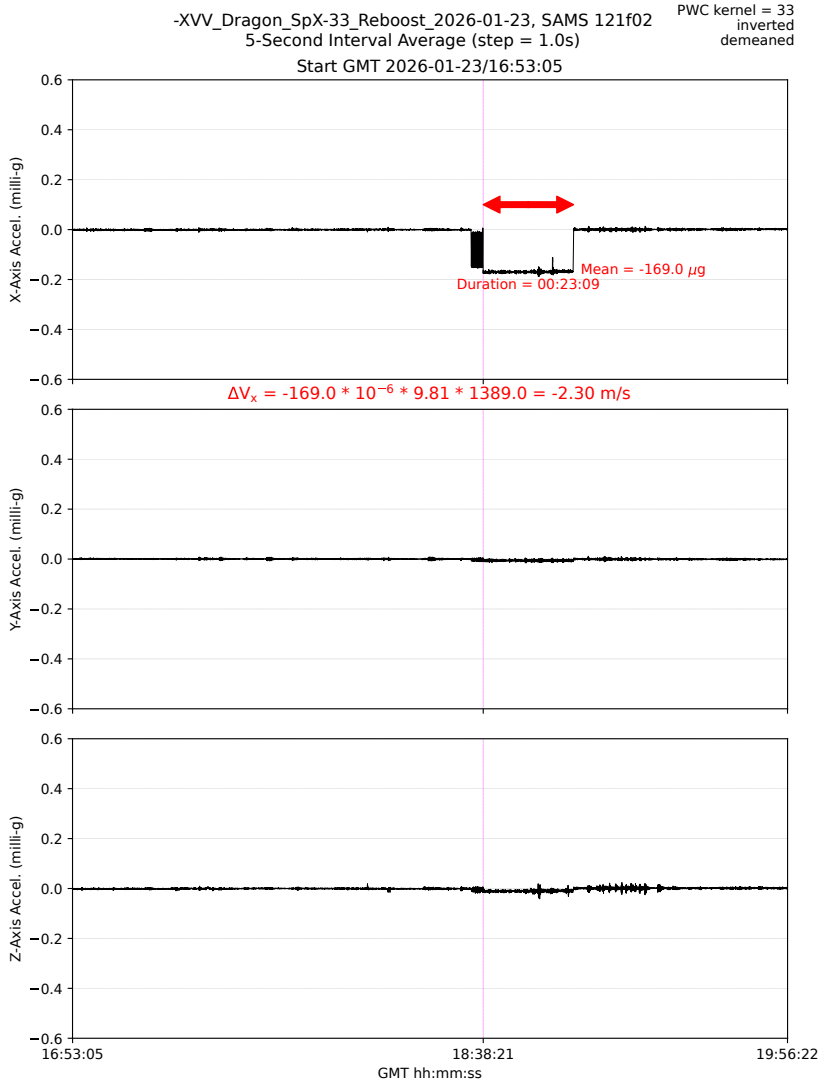

Fig. 13: 5-sec interval average for SAMS 121f02 sensor in COL on the Endcone.

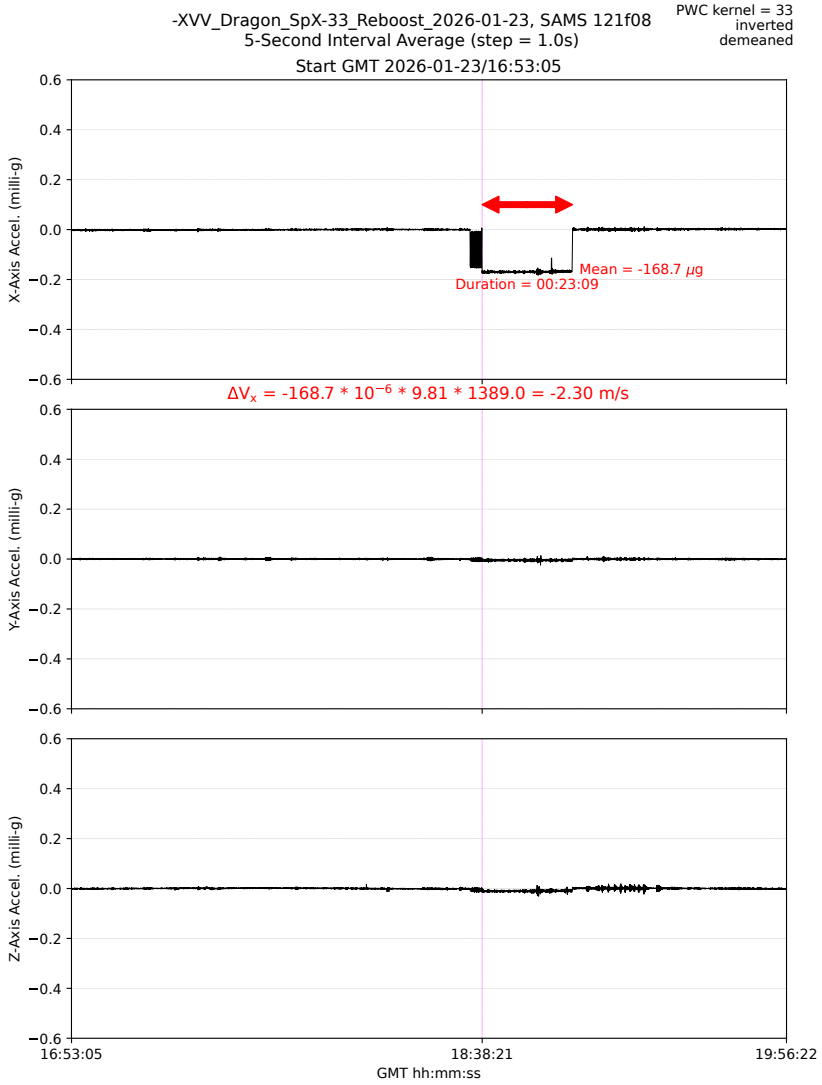

Fig. 14: 5-sec interval average for SAMS 121f08 sensor in COL on COL1A3 Rack.

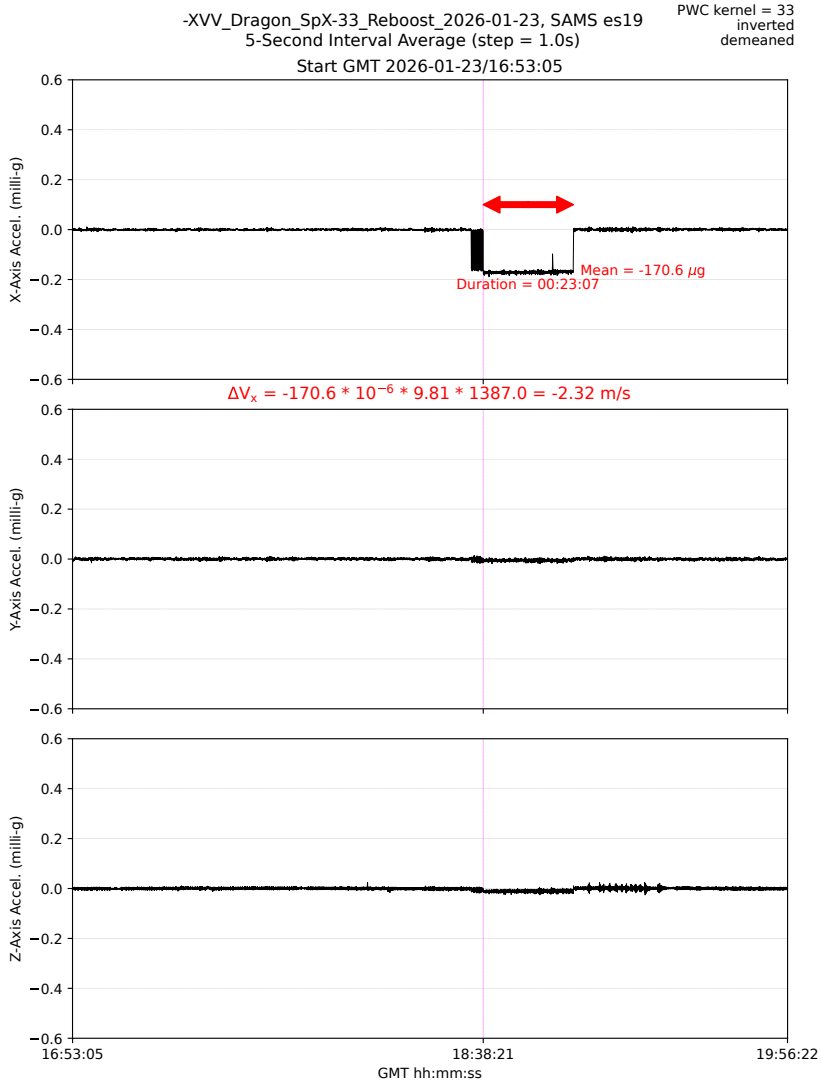

Fig. 15: 5-sec interval average for SAMS es19 sensor in JEM on JPM1F6 (ER4).

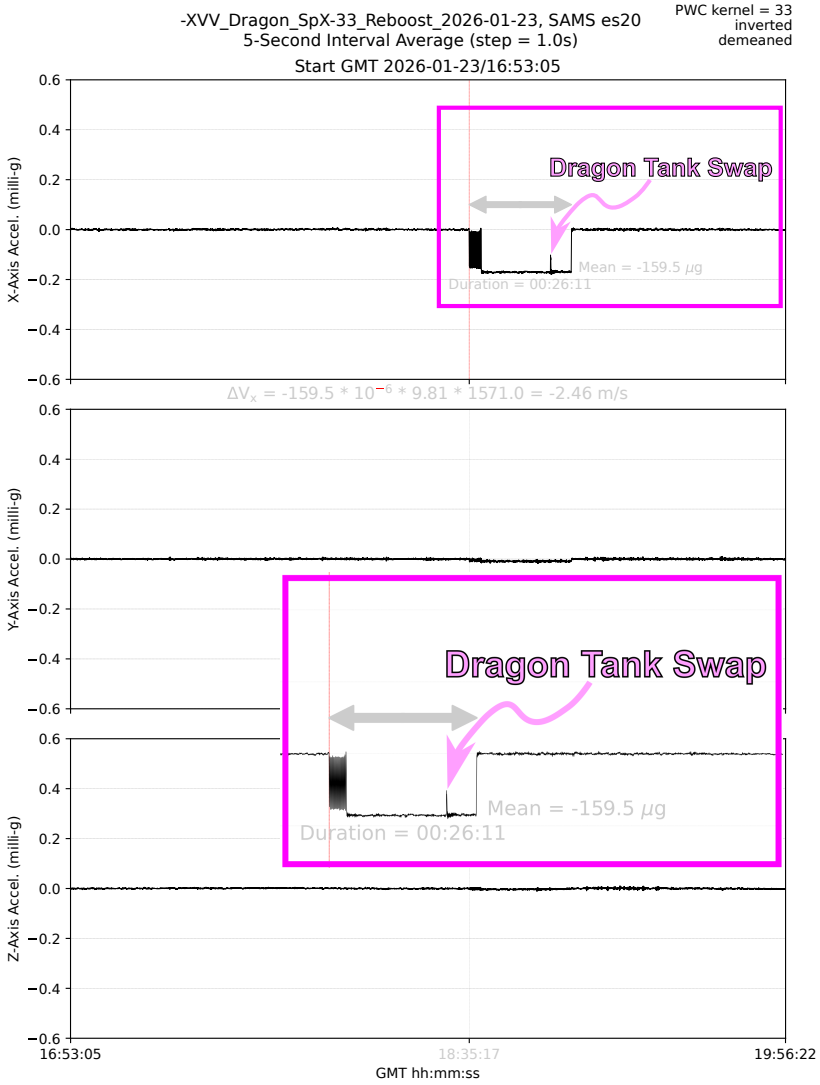

Fig. 16: 5-sec interval average for SAMS es20 sensor at LAB1S2 (MSG).

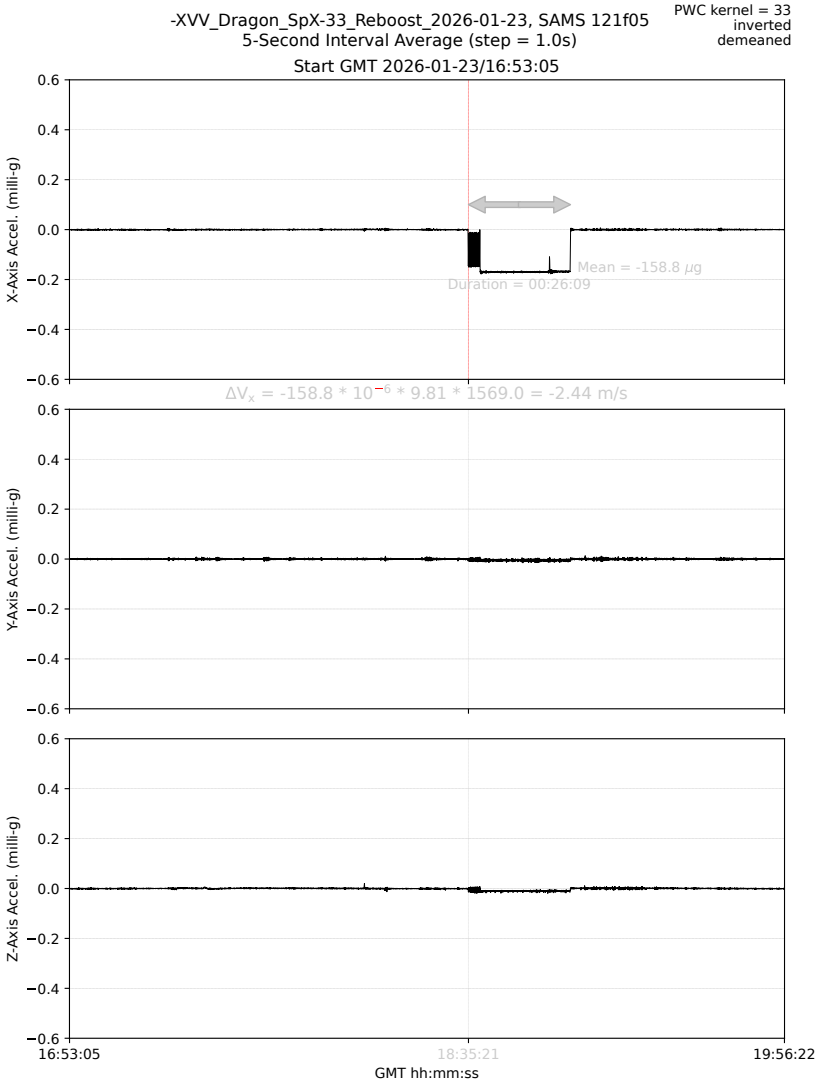

Fig. 17: 5-sec interval average for SAMS 121f05 sensor at JPM1F1 (ER5).

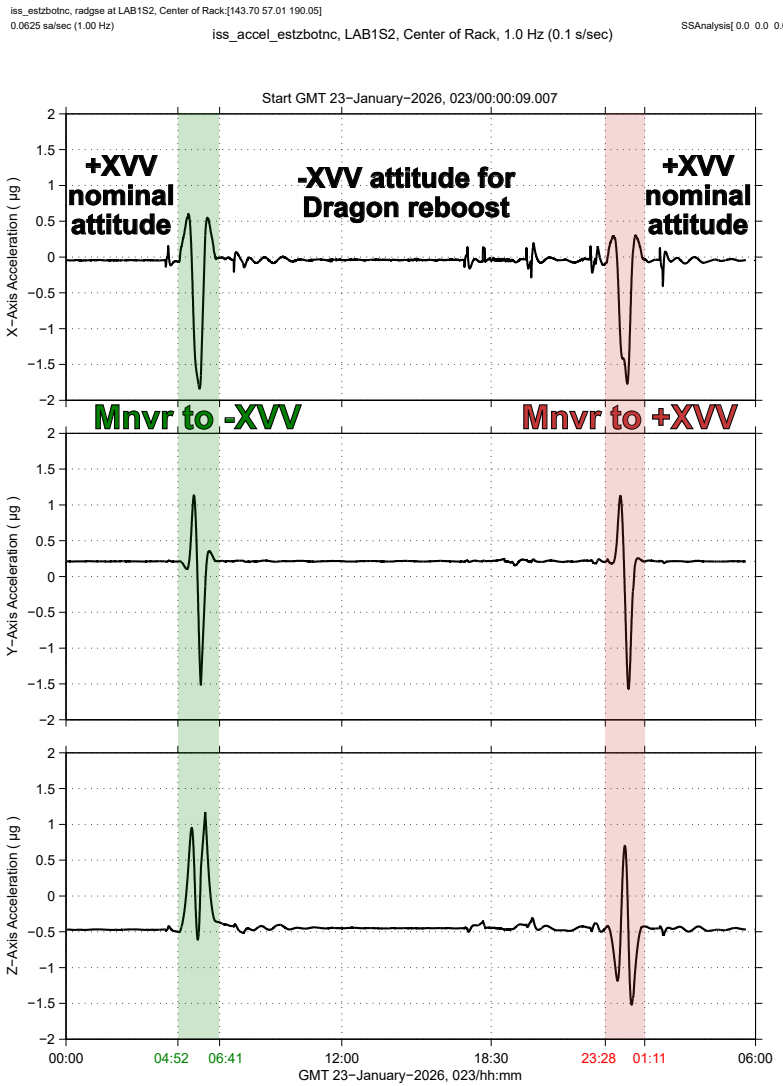

Fig. 18: Estimated Quasi-Steady Accel. vs Time Shows 2 OPM Maneuvers.

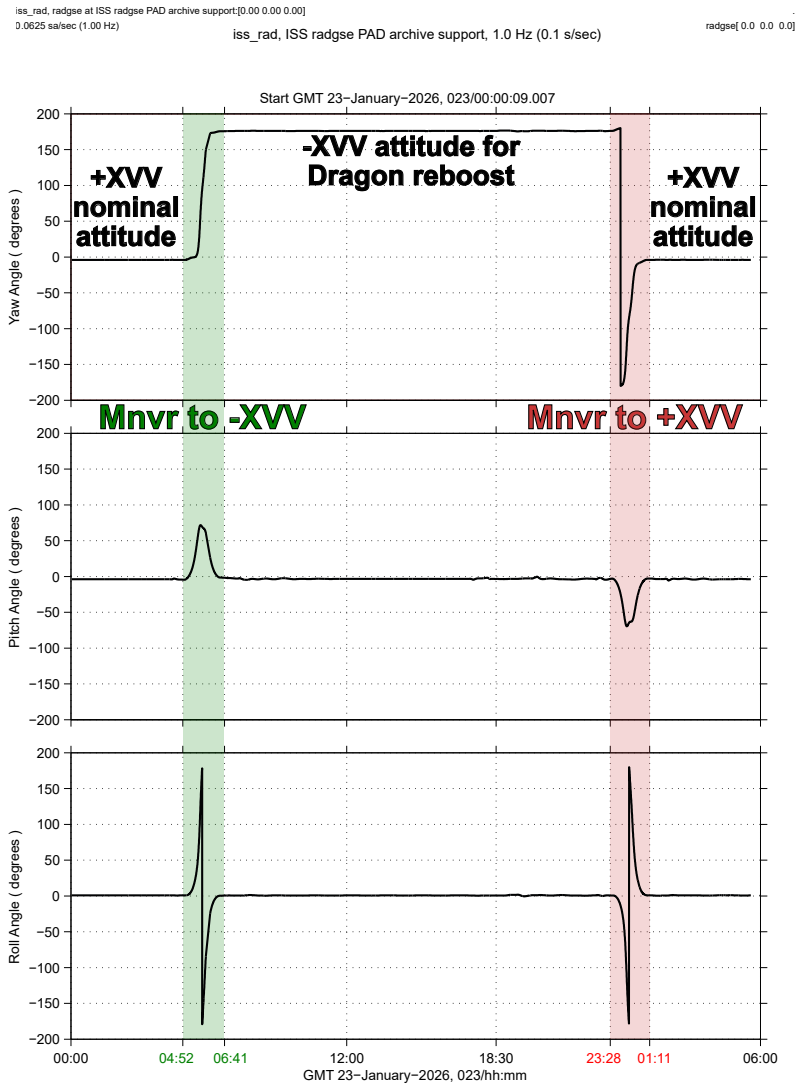

Fig. 19: Space Station Yaw/Pitch/Roll Angles vs. Time Shows 2 OPM Maneuvers.